



مجلة التربوي  
Journal of Educational  
ISSN: 2011- 421X  
Arcif Q3

معامل التأثير العربي 1.5  
العدد 19



# مجلة التربوي

## مجلة علمية محكمة تصدر عن كلية التربية

# جامعة المرقب

العدد التاسع عشر  
يوليو 2021م

هيئة تحرير  
مجلة التربوي

- المجلة ترحب بما يرد عليها من أبحاث وعلى استعداد لنشرها بعد التحكيم .
  - المجلة تحترم كل الاحترام آراء المحكمين وتعمل بمقتضاها .
  - كافة الآراء والأفكار المنشورة تعبر عن آراء أصحابها ولا تتحمل المجلة تبعاتها .
  - يتحمل الباحث مسؤولية الأمانة العلمية وهو المسؤول عما ينشر له .
  - البحوث المقدمة للنشر لا ترد لأصحابها نشرت أو لم تنشر .
- (حقوق الطبع محفوظة للكلية)



### ضوابط النشر:

- يشترط في البحوث العلمية المقدمة للنشر أن يراعى فيها ما يأتي :
- أصول البحث العلمي وقواعده .
  - ألا تكون المادة العلمية قد سبق نشرها أو كانت جزءا من رسالة علمية .
  - يرفق بالبحث تزكية لغوية وفق أنموذج معد .
  - تعدل البحوث المقبولة وتصحح وفق ما يراه المحكمون .
  - التزام الباحث بالضوابط التي وضعتها المجلة من عدد الصفحات ، ونوع الخط ورقمه ، والفترات الزمنية الممنوحة للتعديل ، وما يستجد من ضوابط تضعها المجلة مستقبلا .

### تنبيهات :

- للمجلة الحق في تعديل البحث أو طلب تعديله أو رفضه .
- يخضع البحث في النشر لأولويات المجلة وسياساتها .
- البحوث المنشورة تعبر عن وجهة نظر أصحابها ، ولا تعبر عن وجهة نظر المجلة .

### Information for authors

- 1- Authors of the articles being accepted are required to respect the regulations and the rules of the scientific research.
- 2- The research articles or manuscripts should be original and have not been published previously. Materials that are currently being considered by another journal or is a part of scientific dissertation are requested not to be submitted.
- 3- The research articles should be approved by a linguistic reviewer.
- 4- All research articles in the journal undergo rigorous peer review based on initial editor screening.
- 5- All authors are requested to follow the regulations of publication in the template paper prepared by the editorial board of the journal.

### Attention

- 1- The editor reserves the right to make any necessary changes in the papers, or request the author to do so, or reject the paper submitted.
- 2- The research articles undergo to the policy of the editorial board regarding the priority of publication.
- 3- The published articles represent only the authors' viewpoints.





## Effect Mesoporous silica silver nanoparticles on antibacterial agent Gram-negative *Pseudomonas aeruginosa* and Gram-positive *Staphylococcus aureus*

<sup>1</sup>Hanan B. Abousittash, <sup>2</sup>Z. M. H. Kheiralla and <sup>3</sup>Betiha M.A.

<sup>1</sup>Faculty of Science - Elmergib University, <sup>2</sup>Faculty of Women for Arts, Science, Cairo, Egypt, <sup>3</sup>Egypt Refining Division, Egyptian Petroleum Research Institute, Cairo, Egypt  
habostash@gmail.com

### الخلاصة

تم دراسة النشاط الميكروبي لجزيئات mesoporous Ag/NH<sub>2</sub>-KIT-6(x) النانوية المصنعة بطريقة الأختزال الكيميائي ضد سلالتين من البكتيريا السالبة والموجبة لصبغة جرام هما *S.aureus* و *P.aeruginosa* وأكدت النتائج المتحصل عليها القدرة العالية لجزيئات Ag/NH<sub>2</sub>-KIT-6(x) النانوية بمختلف تركيزات الفضة بها على تثبيط النمو الميكروبي لكلا من *S.aureus* و *P.aeruginosa* مقارنة بالمضادات الحيوية التي تم إستخدامها.

كما لوحظ وجود إختلاف في درجة حساسية كلا الميكروبين للجزيئات النانوية وربما يعود هذا إلى إختلاف تركيب الجدر الخلوية لكلاهما ولهذه الميكروبات أضرار كبيرة حيث أنها من الميكروبات الممرضة للإنسان لإرتباطها بالعديد من الأمراض الجهازية ويتضح من صور الميكروسكوب الماسح مدى التلف التي أحدثته جزيئات Ag/NH<sub>2</sub>-KIT-6(x) النانوية للأغشية الميكروبية الخلوية.

نأمل في المستقبل إستخدام أنواع مصنعة ونقية من الجزيئات النانوية في صورة silica mesoporous لعلاج الالتهابات البكتيرية المقاومة للأدوية التي تسببها الأغشية الحيوية.

### Abstract

Increase more attention to eco-friendly mesoporous silica silver nanoparticles featuring smaller particle sizes to enhance their remarkable antimicrobial properties. A simple chemical method was developed for synthesize high valence silver nanoparticles immobilized on the mesoporous silica nanomaterial, which showed strong antibacterial activity. Chemical reduction of silver ion has been regarded in the present work, and a



reducing agent , such as hydrazine was used to promote the reduction of the silver ion – precursor. The average particle size of the synthesized mesoporous silica-silver nanoparticles (Ag/NH<sub>2</sub>-KIT-6(x)) with different concentrations of Ag (2.5 and 7%) calculated from Scherrer's equation for (1 1 1)-plane were 8 and 6.5 nm respectively. The synthesized materials were characterized using FTIR spectra, X-Ray diffraction (XRD), X-ray photoelectron spectroscopy (XPS) and transmission electron microscopy (TEM), which revealed the mesoporous silica nanoparticles.

Antibacterial activities of mesoporous silica silver nanoparticles against Gram- negative *Pseudomonas aeruginosa* and Gram-positive *Staphylococcus aureus* were found to be increased with the increasing of Ag concentration in the Ag/NH<sub>2</sub>-KIT-6(x). The maximum inhibition zone diameter when the concentration 7 % was used obtained against *P. aeruginosa* and *S. aureus* with diameters of 33 and 30 mm respectively. The antimicrobial activity of mesoporous Ag/NH<sub>2</sub>-KIT-6(x) was evaluated also using the MIC&MBC tests. Biofilm forming from a variety of microbial pathogens can pose a serious health hazard that is difficult to combat. Nanotechnology, however, represents a new approach to fighting and eradicating biofilm-forming microorganisms. The biofilm formation by microplate method of both the untreated and the treated bacterial cells. Scanning electron microscopy observations clearly indicate that silver nanoparticles reduced the surface coverage by *P.aeruginosa* and *S. aureus*. thus prevent the biofilm formations. Mesoporous Ag/NH<sub>2</sub>-KIT-6 (7 %) exhibited excellent antibiofilm activity and prevented biofilm formation by *P.aeruginosa* and *S. aureus*. In conclusion the use of silver nanoparticles as antibacterial agent was according to be toxic against pathogenic bacteria and considered advantageous over other methods for control of pathogenic microorganisms, and it can be of great importance in developing novel drugs for curing many lethal diseases.

## Introduction

**Klevens et al. (2007) and Walker et al. (2009)** increasing hospital and community-acquired infections due to bacterial multidrug-resistant (MDR) pathogens for which current antibiotic therapies are not effective and represent a growing problem. Antimicrobial resistance and biofilm development in affected patients is thus one of the major threats to human health, since it determines an increase of morbidity and mortality as a consequence of the most common bacterial diseases.

**(Ruedas-Rama et al., 2012; Yildirim et al., 2013; Natarajan and Chen et al., 2014 and Selvaraj, 2014)** mesoporous silica nanoparticles (MSNs) are well known for their biocompatibility, dispersibility, and chemical stability as carriers for drug/gene/antimicrobial agents. They have also been used as cell markers, catalytic substrates, absorbents, and matrix fillers. They can be synthesized with controlled size, shape and varying textural properties (e.g. pore size, surface area and porosity) for therapeutic uses **(Wu et al., 2013 and Qasim et al., 2014)**. Porous materials are of great interest because of their ability to interact with atoms, ions, molecules and nanoparticles not



only at their surfaces, but throughout the bulk of the materials. Therefore, the presence of pores in nanostructured materials greatly promotes their physical and chemical properties (**Han et al., 2011**).

**Rai et al. (2012)** nanoparticles are now considered a viable alternative to antibiotics and seem to have a high potential to solve the problem of the emergence of bacterial multidrug resistance. Metal nanoparticles of silver, copper, and gold have been according to be active against certain pathogenic bacteria and fungi. In particular, silver nanoparticles have attracted much attention in the scientific field.

**Taraszkiewicz et al. (2012) and Franci et al. (2015)** silver has always been used against various diseases, in the past it was used as an antiseptic and antimicrobial against Gram-positive and Gram-negative bacteria. Comparatively, silver nanoparticles have been intensely studied owing to their distinct properties such as conductivity, chemical stability, catalytic activity, nonlinear optical behavior, low cytotoxicity and strong inhibitory and bactericidal effects as well as a broad spectrum of antimicrobial activities. These properties make them suitable for use as an antimicrobial agent in catheters, burns, severe chronic osteomyelitis, urinary tract infections and medical textiles.

**Sweet and Singleton, 2011 and Rai et al. (2016)** mesoporous silica silver nanobartecal were considered, particularly attractive for the production of a new class of antimicrobials opening up a completely new way to combat a wide range of bacterial pathogens. The production of mesoporous Silica - AgNPs is relatively inexpensive and the addition of these particles into goods such as plastics, clothing, creams, and soaps increase their market value (**Feng et al., 2000**). The aim of the work presents an overview of mesoporous silica-silver nanoparticles preparation by chemical methods and the implications of their use in controlling pathogenic microbes as they were tested for their antibacterial efficacy for different multidrug-resistant bacterial strains.

## Materials and Methods:

### Chemicals

Pluronic P123 (triblock copolymer P123,  $\text{EO}_{20}\text{PO}_{70}\text{EO}_{20}$ , Mw of  $\approx 5800$ ), tetraethyl orthosilicate (TEOS,  $\geq 99.0\%$ ), 3-Aminopropyltrimethoxysilane (APTS, 97%), 2,4,6-trinitrobenzenesulfonic acid (TNBS, 1 M in  $\text{H}_2\text{O}$ ), potassium tetraborate tetrahydrate ( $\text{K}_2\text{B}_4\text{O}_7$ ,  $\geq 99.5\%$ ), tetrabutylammonium bromide ( $\geq 98\%$ ), 1-butanol ( $\geq 99\%$ ), HCl (35wt. %), hydrazine hydrate, silver acetate (99.99%), 1,2,4-trimethylbenzene solvents including methanol and ethanol were purchased from Sigma-Aldrich and used without further purification.

### Synthesis of High Valence of Mesoporous Silica Silver Nanoparticles

Reported by **Qian et al. (2012) and Hassan et al. (2016)** the KIT-6 was synthesized with some modification. Ten g of Pluronic P123 were melted ( $75^\circ\text{C}$ ) and then dissolved in



300 ml distilled water and 35 ml HCl (35 wt. %). The mixture was sheared at 350 rpm for 1 h. at 35°C then, 10 ml of 1-butanol and 1 ml of 1, 2,4-trimethylbenzene were added at once to the stirred mixture for 30 min. at 35°C. After that, 20 g of TEOS was added to the stirred mixture and it was further stirred for 24 h. at 35°C. Then, the mixture was transferred to 500 ml Teflon autoclave and the hydrothermal process was carried out for 48 h. at 130°C under static conditions. The dried obtained white material after filtration and washing with mixture of water and ethanol was finally calcined in air atmosphere at 600 °C for 8 h.

**Hassan *et al.* (2014)** the obtained free surfactant KIT-6 was coupled with APTS to functionalize the KIT-6 pores with propylamine moieties as following, 2.0 g of APTS was added directly to 5.0 g of degassed KIT-6 in 150 ml dry toluene under mechanical stirring for 4 h, at ambient temperature and then refluxed for another 12 h. The obtained material NH<sub>2</sub>-KIT-6 was recovered by centrifuge, washed several times with ethanol-water mixture (50/50 V/V) to remove unreacted APTS molecules and vacuum dried at 60°C overnight.

**Weber *et al.* (2000)** the amino groups functionalized KIT-6 was determined gravimetrically by using, 2, 4, 6-trinitrobenzenesulfonic acid. The degassed NH<sub>2</sub>-KIT-6 (0.1 g) was suspended in double distilled water (1 ml) at 50°C for 2 h and left to cool. Then, the suspended NH<sub>2</sub>-KIT-6 was further diluted with 5 ml of 100 mmol borate buffer (K<sub>2</sub>B<sub>4</sub>O<sub>7</sub>; pH=9.3), and 1.5 ml of 1000 mmol TNBS solution was added and allowed to react for 4 h at 35 °C. After that, the NH<sub>2</sub>-KIT-6 was recovered by centrifuge at 14000 rpm for 5 min. The supernatant absorption was measured at 350 nm to determine the concentration of TNBS molecules. Reference samples were prepared in parallel composed of 6 ml of double distilled water of K<sub>2</sub>B<sub>4</sub>O<sub>7</sub> material without NH<sub>2</sub>-KIT-6 material, and the concentration of amino was confirmed with TNBS solutions.

The doping of silver nanoparticle on NH<sub>2</sub>-KIT-6 at different loading were prepared in dry toluene using tetrabutylammonium bromide as cationic surfactant and silver acetate as a silver precursor. Briefly, 1.0 g of NH<sub>2</sub>-KIT-6 (1.628 mmol of –NH<sub>2</sub>) was suspended in 10 ml of toluene under ultrasonic irradiation for 15 min, and 5 ml of aqueous containing 0.25% tetrabutylammonium bromide and 6 µl of hydrazine are added and the mixture was further sonicated for additional 5 min. A 0.138 g (0.81 mmol) of silver acetate in 5 ml of distilled water was injected into the sonicated mixture under vigorous stirring. The mixture color slowly turned from white to pink, ruby and dark red color, confirming formation of silver nanoparticles. The mixture temperature is raised to 45°C to ensure the compellation of reaction for 2 h, and the solvents were drained under vacuum at 80°C. After solidification, the obtained sample was washed several times with water-ethanol (90/5; V/V) until free tetrabutylammonium bromide was detected by AgNO<sub>3</sub>. Finally, the obtained sample was dried under vacuum for 6 h. silver nanoparticles immobilized in NH<sub>2</sub>-KIT-6 was stirred in 10 % HNO<sub>3</sub> and analyzed by Inductive Coupled Plasma (ICP). The samples were donated as Ag/NH<sub>2</sub>-KIT-6(x), where x represents the weight ratio of Ag<sup>0</sup> immobilized on NH<sub>2</sub>-KIT-6 2.5 and 7 %.



## Characterization of Mesoporous Silica Silver Nanoparticles

**McCusker and Baerlocher, (2001) and Rai and Duran, (2011)** the XRD patterns were performed in X'Pert PRO instrument using Cu K $\alpha$  radiation at 40 kV and 30 mA. In powder XRD patterns, the positions of the peaks are determined only by the dimensions and shape of the unit cell and in general the intensities depend on the type of atoms and their position within the unit cell. Diffractograms were obtained from 0.5 to 10 ( $2\Theta$ ) at a scanning speed of 0.05 deg. min<sup>-1</sup> and counting time of 5 s.

The N<sub>2</sub>-adsorption isotherms were performed at -196 °C in NOVA 3200 system instrument. The specific surface area was measured by applying the BET equation to the adsorption isotherm in regime  $\geq 0.35$  of P/P<sub>0</sub> value. The pore size distribution was calculated from Barrett–Joyner–Halenda (BJH) method. The total pore volume was considered to be the volume of liquid N<sub>2</sub> adsorbed at a relative pressure of 0.98. Prior to the analysis, the samples were outgassed under vacuum at 140°C for at least 16 h. High Resolution Transmission Electron Microscope images were obtained on a JEOL JEM 2100 microscope. Transmission Electron Microscope samples were prepared by sonication of the powder in ethanol and evaporating one drop onto a holey carbon film.

The FTIR spectra were recorded on a Nicolet iS10 Fourier transform infrared spectrophotometer. X-ray photoelectron spectroscopy (XPS) was carried out using a Thermo Scientific K-ALPHA USA instrument equipped with a dual X-ray source, using the AlK $\alpha$  radiation anode and a hemispherical energy analyzer. With an analyzer chamber pressure of 10<sup>-9</sup> torr at a power of 250W. Metal's concentration impregnated in the samples was quantitatively determined using standard methods of analyses including Inductive Coupled Plasma (ICP). The ICP instrument is ICP-OES Perkin-Elmer Optima 2000 DV.

## Microbiological Experiments:

### Bacterial cultures

Two experimental bacterial strains, Gram positive *Staphylococcus aureus* and Gram negative *Pseudomonas aeruginosa* in addition were used in this study was isolated from hospitalized patients with indwelling catheter suffering from urinary tract infections (UTIs) by applying the standard methods of Harley . Bacterial cultures and Prescott (2002). Preserved at 4°C on nutrient agar slants. Colonies were identified by gram staining according to the conventional method, and the biochemical tests were done using API 20 test kits (bioMérieux, Inc., France).

### Antibacterial susceptibility testing

Eight different antibiotics including Cefotaxime 30 $\mu$ g, Ceftriaxone 75 $\mu$ g, Amikacin 10 $\mu$ g, Nalidixic acid 30 $\mu$ g, Neomycin 30 $\mu$ g, Sulfamethoxazole-trimethoprim 25 $\mu$ g, Ampicillin 30 $\mu$ g and Colifuran 200 $\mu$ g as standard antibacterial agents were used and antibacterial



susceptibility test was performed by disk diffusion method on Mueller–Hinton agar plates according to **Kheiralla et al. (2014)**.

### **Assessment of the antibacterial activity of mesoporous silica silver nanoparticles well diffusion method**

The antibacterial susceptibility of strains was determined by agar well diffusion method as described by Abbaszadegan *et al.* (2015) Briefly, colonies from an overnight culture of the tested bacteria grown on nutrient agar were suspended in saline and turbidity was adjusted to 0.5 McFarland ( $1 \times 10^8$  CFU/ml). Plates of Mueller–Hinton agar were inoculated using a sterile swab to produce a confluent lawn of growth. Using sterile cork borer, the well (6 mm) was made into each Petri. A 50 ml of AgNPs suspended into dimethyl sulfoxid DEMSO 100  $\mu\text{g/ml}$  to was added into the wells, then the plates were left at refrigerator for 3 hours to allow diffusion of the test sample and incubated at 37°C for 24 hours after which zones of inhibition were measured.

### **Minimum inhibitory concentration (MIC) and minimum bactericidal concentration (MBC) Test:**

The minimum inhibitory concentration (MIC) was defined as the lowest concentration of antimicrobial agents that inhibited 90 percent of the bacterial growth after an overnight incubation in comparison with the negative control **Abbaszadegan et al. (2015)**. The minimum inhibitory concentration and MIC of silver nanoparticles were assessed by the macro dilution broth susceptibility test according to the method based on the US National Committee for Clinical Laboratory Standards Guidelines **Kheiralla et al. (2014)** and **Karthikeyan et al. (2011)**. Sterile Mueller–Hinton broth was used as diluents for the preparation of silver nanoparticles dilution. A serial dilution of the 0.01mg/ml silver nanoparticles solution was prepared within a desired range. One milliliter of each bacterial suspension that was prepared by suspending colonies from an overnight cultured tested bacteria on nutrient agar in sterile saline solution (0.85% NaCl) and adjusting turbidity to 0.5 McFarland ( $1 \times 10^8$  CFU/ml) was inoculated and then tubes were incubated for 24 h. at 37°C, the control tubes without the silver nanoparticles were assayed simultaneously. To test the bactericidal effect a loopful from each tube was inoculated on Mueller–Hinton agar and incubated for 24 h. at 37°C. **Ruparelia et al., (2008)** the nanoparticles concentration causing bactericidal effect was selected based on absence of colonies on the agar plate. The results were plotted as the mean value of 3 mutually independent experiments.

### **Effect of mesoporous silica silver nanoparticles on the biofilm formation of bacterial by microplate method:**

The effects of mesoporous silica silver nanoparticles on the morphology of both *P. aeruginosa* and *S. aureus* were tested for biofilm formation. Bacterial strains were grown overnight in Trypticase Soy broth (TSB) supplemented with 0.25% glucose at 37°C. After





that, the strains were diluted 1/200 in TSB supplemented with 0.25% glucose and 200 µl of this suspension was inoculated in triplicate to polystyrol microliter plates to them 100 µl of DEMSO containing 1µg of mesoporous silica silver nanoparticles (7% ) was added treated also bacterial suspension were inoculated in triplicate without nanoparticles untreated and incubated overnight at 37°C. Then, the cellswere decanted and wells were washed three times with phosphate buffer (PB), dried at room temperature and finally stained with 0.1% safranin. Absorbance of the adherent cells was measured at 490 nm using a microplate reader (Mindray, MR-96A). A strain was considered positive, if its absorbance value was > 0.12 (Christensen *et al.* 1985).

### Statistical analysis

(SPSS, 2006) the experiments were replicated three independent times and the data are presented as mean ±STD. Statistical analysis was carried out using Student's t test. Differences were considered statistically significant when P-value was less than 0.01.

After testing the data for normality, the differences in the treatments were tested using one-way analysis of variance (ANOVA 1) according to SPSS software. A post-hoc test was applied when differences were significant.

### Results and Discussion

Yuan *et al.* (2017) overuse or misuse of antimicrobial agents has led to the development of multi-drug resistant bacteria. To overcome the limitations of conventional synthetic antimicrobial compounds, nanotechnology represents an alternative strategy in developing alternative antimicrobial agents that can efficiently kill bacterial cells and display immense potential for use in both medical and veterinary applications

### Characterization of Mesoporous Silica Silver Nanoparticles

The sol-gel technique is one of the most important facile methods for porous preparation materials. The ordered cubic pore of silicate was synthesized using TEOS as silica precursor, HCl as a hydrolysis catalyst, P123 as structure directing agent (PO moieties as phase separation inducers; PEO moieties as a gelling agent) and butanol as co-surfactant. The pore construction morphology is determined by the balance between the silica coarsening and the structure freezing by P123 and butanol co-surfactant that create the cubic morphology of the obtained monolithic silica. The second phase includes grafting of APTS on the silica in toluene, forming covalent bond between the monolithic silica and amino-organosilane moieties (Fig. 1). After that, the obtained amino-silicate (NH<sub>2</sub>-KIT-6) was used as a platform to cap the reduced silver nanoparticle. In this stage, the silver acetate was embedded on NH<sub>2</sub>-KIT-6, forming an Ag-NH<sub>2</sub>-SiO<sub>2</sub> complex, and an appropriate amount of hydrazine was used to promote the decrease of the silver complex.

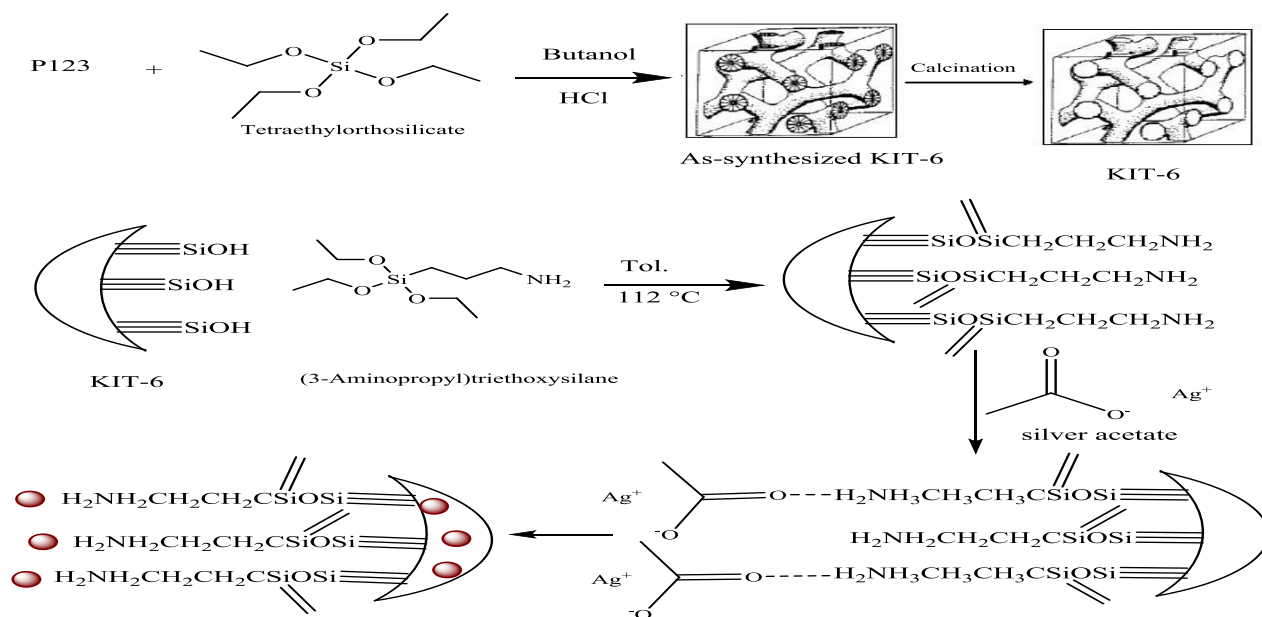


**Fig.1:** Schematic representation of the preparation of KIT-6, NH<sub>2</sub>-KIT-6 and Ag/NH<sub>2</sub>-KIT6(x).

The concentration of amino group per gram was of 1.45 mmol g<sup>-1</sup> and the immobilized silver according to ICP analysis was of 7% and 2.5%, for Ag/NH<sub>2</sub>-KIT-6(7 %) and Ag-NH<sub>2</sub>-KIT-6(2.5%). The FTIR assembly details of the KIT-6 functionalized NH<sub>2</sub>-KIT-6 and Ag/NH<sub>2</sub>-KIT-6(x), were examined. Spectra of NH<sub>2</sub>-KIT-6 and Ag immobilized on Ag-NH<sub>2</sub>-KIT-6(7&2.5%) are shown in **Fig. 2** The KIT-6, NH<sub>2</sub>-KIT-6 and Ag/NH<sub>2</sub>-KIT-6 (7 and 2.5 %) exhibit the characteristic stretching broad bands associated with ≡Si-OH groups in the regime of 3450–3350 cm<sup>-1</sup>, while the corresponding binding band for KIT-6 & NH<sub>2</sub>-KIT-6, are observed at 1665 cm<sup>-1</sup> and 1650 cm<sup>-1</sup> for Ag/NH<sub>2</sub>-KIT-6. The NH<sub>2</sub>-KIT-6 exhibits the characteristic -CH<sub>2</sub> asymmetric and symmetric stretching bands near 2933 cm<sup>-1</sup> and 2821 cm<sup>-1</sup>, respectively. While asymmetric Si-O-Si stretching bands appeared near 1066 cm<sup>-1</sup>, the band near 969 cm<sup>-1</sup> is due to the Si-O bending in the Si-OH groups and asymmetric Si-O-Si stretching band appeared near 810 cm<sup>-1</sup>. The vibration band at 3137 cm<sup>-1</sup> in NH<sub>2</sub>-KIT-6 is attributed to the stretching vibration of -NH<sub>2</sub> that is in hydrogen bonding with Si-OH. The presence of asymmetric -N-H bending vibration near 707 cm<sup>-1</sup> confirms the incorporation of an amino group on the KIT-6 material. The band at 1380 cm<sup>-1</sup> associated with -CH<sub>2</sub> vibration, can be seen for the samples containing aminopropyl groups containing silver metal (Coates, 2000 and Wang *et al.*, 2005). However this band became more intense as Ag loading increase, implying free mobility of propylamine moieties after deposition Ag<sup>0</sup> on -Si-OH.

(Sajab *et al.*, 2011) Furthermore, the significant reduction in band intensities at 3450–3350 cm<sup>-1</sup>, conforming consumption of hydroxyl group after Ag anchoring in NH<sub>2</sub>-



KIT-6 surface, suggesting that portion of silver acetate is incorporated on  $-\text{SiO}_2$  moieties. Finally, the intensity of the characteristic absorption bands in the range  $1350\text{--}960\text{ cm}^{-1}$  are also observed for all the samples, indicating slight changes in the pore structures after adsorption, which may be because of inherent disorder in the virgin and functionalized material structures.

The low angle XRD patterns of KIT-6,  $\text{NH}_2\text{-KIT-6}$  and  $\text{Ag/NH}_2\text{-KIT-6}$ (2.5 and 7%) are shown in **Fig.3** The KIT-6 and  $\text{NH}_2\text{-KIT-6}$  samples exhibit three well-resolved; one strong intense diffraction peak and two minor diffraction peaks that assigned to (2 1 1), (2 2 0) and (3 3 2) reflections, which can be indexed to  $Ia\bar{3}d$ , suggesting high ordered cubic mesoporous structure. It is clear that the intense peaks are shifted to lower angle after grafting APRTS molecule and more shift is noticed after  $\text{Ag}^+$  loading. This behavior is resulted from increase the pore wall due to the grafting  $\text{Ag}^0$  on propylamine moieties. In addition, the  $a_0$  (unit cell parameter) is increased after  $\text{Ag}^0$  immobilization on KIT-6, escorted by the shift of the intense peak (2 1 1) reflection to lower angle. The high angle XRD patterns of KIT-6,  $\text{NH}_2\text{-KIT-6}$ ,  $\text{Ag/NH}_2\text{-KIT-6}$ (2.5, 7 %), are shown in **Fig. 4**. The XRD patterns of KIT-6 and  $\text{NH}_2\text{-KIT-6}$  showed broad peak centered at  $23.11^\circ$ , while very weak peaks of the  $\text{Ag}^0$  species in  $\text{Ag/NH}_2\text{-KIT-6}$ (2.5) materials is detected due to the high dispersion of silver on  $\text{NH}_2\text{-KIT-6}$ , while four peaks at  $38.04^\circ$ ,  $44.29^\circ$ ,  $64.30^\circ$  and  $77.39^\circ$  corresponding to (1 1 1), (2 0 0), (2 2 0) and (3 1 1) plane-reflections of fcc  $\text{Ag}^0$  nanostructure is noticed for  $\text{Ag/NH}_2\text{-KIT-6}$ (2.5%) material. The average particles size of AgNPs calculated from Scherrer's equation for (1 1 1)-plane were of 8 and 6.5 nm for  $\text{Ag/NH}_2\text{-KIT-6}$ (7 %) and  $\text{Ag/NH}_2\text{-KIT-6}$ (2.5 %), respectively.

Shown in **Fig. 5** the HRTEM images of the prepared samples . The KIT-6 and  $\text{NH}_2\text{-KIT}$  samples exhibited well 3D cubic ordered mesoporous materials. The  $\text{Ag}^0$  immobilized  $\text{NH}_2\text{-KIT}$  showed ordered/disordered mesopores, however the irregular domains become predominant as  $\text{Ag}^0$  loading increased due to the significant adsorption of  $\text{Ag}^0$  particle on amino or silanol groups. Moreover, the AgNPs appeared highly dispersed on  $\text{NH}_2\text{-KIT}$  and took the direction of KIT-6 pores, and the particle size distribution of silver nanobarticales was of 4-9 nm size.

Shown in **Fig. 6** the  $\text{N}_2$  adsorption-desorption isotherms of KIT-6,  $\text{NH}_2\text{-KIT-6}$  and  $\text{Ag/NH}_2\text{-KIT-6}$ (2.5, 7 %) materials and the textural properties are collected in **Table 1**. All samples displayed Type IV isotherms with pronounced capillary condensation at high relative  $P/P_0$  and H1 hysteresis loop, indicating large uniform channel-like mesoporous with narrow pore size distribution. The BET of KIT-6 was of  $705\text{ m}^2\text{ g}^{-1}$ , however, after grafting APRTS, the surface area decreased to  $503\text{ m}^2\text{ g}^{-1}$ , and the sharp decrease is noticed after immobilization of silver nanobarticales. The BET of  $\text{Ag/NH}_2\text{-KIT-6}$ (2.5, 7%) was of  $315\text{ m}^2\text{ g}^{-1}$  and  $280\text{ m}^2\text{ g}^{-1}$ , implying good dispersion of AgNP in the inter-connected pore of KIT-6.

Shown in **Fig. 7** the UV-Vis absorption of  $\text{NH}_2\text{-KIT}$  and  $\text{Ag/NH}_2\text{-KIT-6}$ (2.5,7%) materials.the bare  $\text{NH}_2\text{-KIT}$ - didn't show any UV-Vis absorption, while  $\text{Ag/NH}_2\text{-KIT-6}$ (2.5



%) and Ag/NH<sub>2</sub>-KIT-6(7 %) showed UV-Vis absorption at 413 nm and 417 nm, respectively due to the Mie Plasmon resonance excitation of silver nanoparticles (**Kim et al., 2006**). As the concentration of silver nanoparticles increased, the Plasmon resonance peak showed slight red shift, indicating the silver nanoparticles particle becomes larger somewhat. However, the low difference in silver nanoparticles particle size is attributed to the chemical coordination and steric effect of amino groups grafted on KIT-6 materials that obstruct the further growth of silver size.

The XPS spectra were used to demonstrate chemical environment for carbon, nitrogen and silver elements **Fig. 8**. The high resolution XPS of C 1s is showed three peaks of binding energy at 284.28, 284.6 and 286.24 eV, appoint to C-C, C-H, and C-N sp<sup>3</sup> carbon, respectively. The XPS spectra in the N 1s binding energy range displayed the spin orbital single for NH<sub>2</sub>-KIT-6 and doublet for Ag/NH<sub>2</sub>-KIT-6(7%) at 399.7 and 401.2 eV, indicating that electron transfer from nitrogen atom to metallic Ag<sup>0</sup>. These values are in agreement the presence of -NH<sub>2</sub> and coordinated -NH<sub>2</sub>, as reported for other immobilized Ag<sup>0</sup>. The XPS profile of Ag 3d is curve-fitted into doublet spin-orbital with ≈6 eV separation, **Ferraria et al. (2010)** centered at 367.6 and 373.5 eV, which assigned to Ag 3d<sub>5/2</sub> and Ag 3d<sub>3/2</sub> present on NH<sub>2</sub>-KIT-6. In this study absence of the peaks at ~368 and ~374 eV indicates that all silver atoms are reduced (**Gebeyehu et al., 2016**).

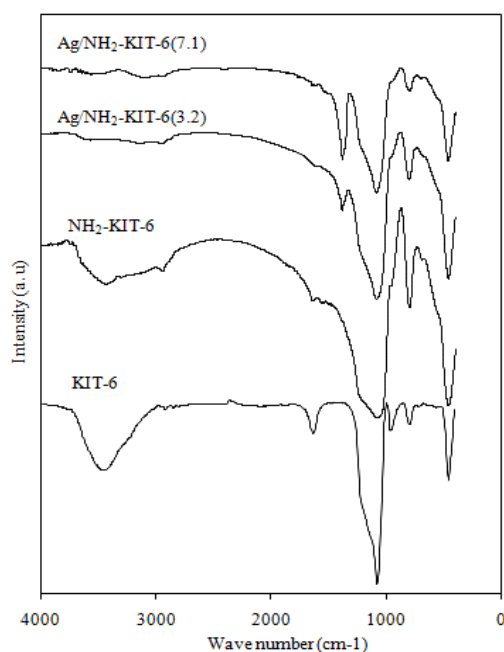


**Fig. 2:** FTIR spectra of calcined KIT-6, NH<sub>2</sub>-KIT-6, Ag/NH<sub>2</sub>-KIT-6 (2.5 & 7%) materials.

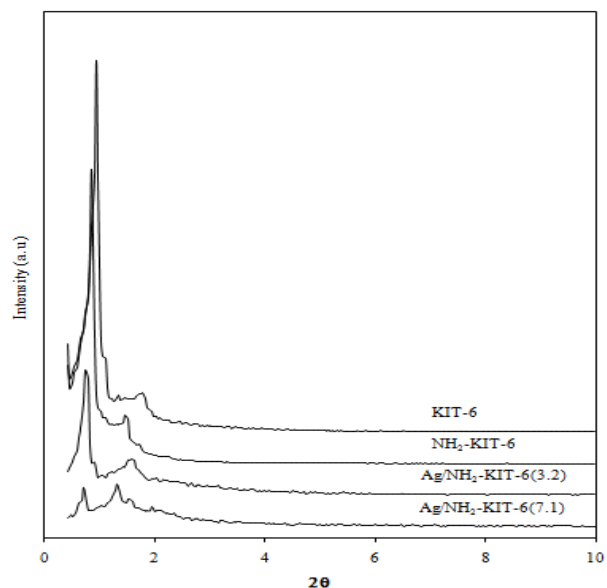


**Fig. 3:** Low XRD patterns for KIT-6, NH<sub>2</sub>-KIT-6 and Ag/NH<sub>2</sub>-KIT-6 (2.5 & 7%) materials.

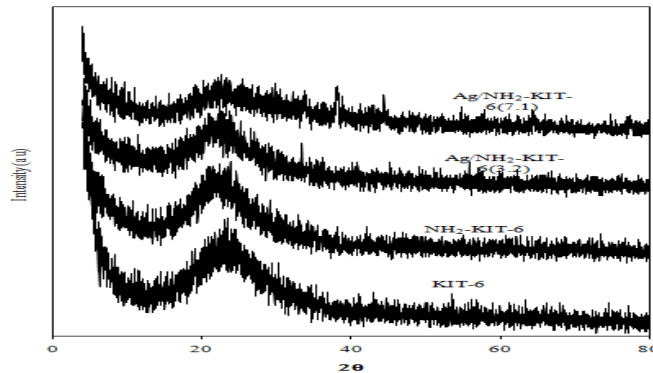


**Fig. 4:** High XRD patterns of KIT-6, NH<sub>2</sub>-KIT-6 and Ag/NH<sub>2</sub>-KIT 6 (2.5 & 7%) materials.

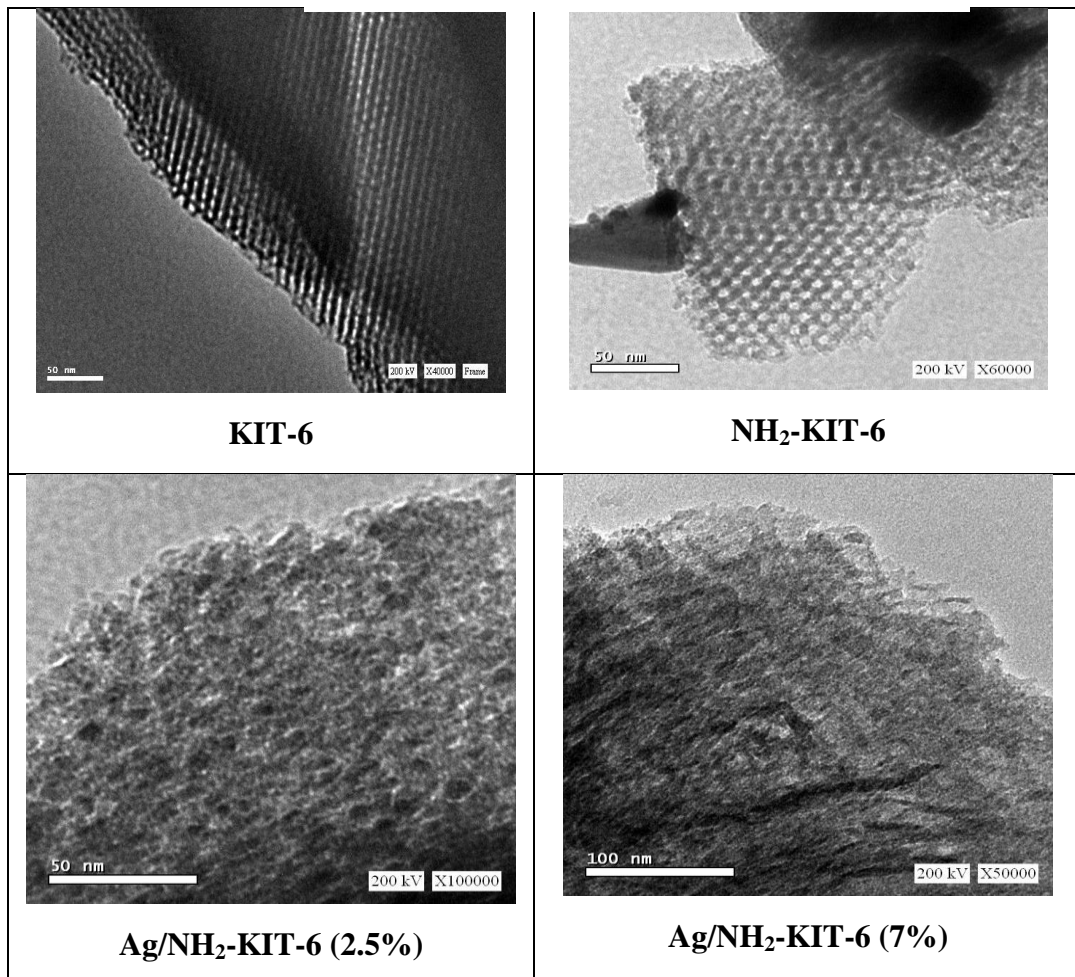


**Fig. 5:** High Resolution Transmission Electron Microscope images of KIT-6, NH<sub>2</sub>-KIT-6 and Ag/NH<sub>2</sub>-KIT-6 (2.5&7%) materials.



**Table 1:** The physicochemical characterization and textural of KIT-6, NH<sub>2</sub>-KIT-6 and NH<sub>2</sub>-KIT-6 (2.5 & 7 %).

Sample	$d_{211}(\text{\AA})$	$a_0$ (nm)	$W_T$	$S_{BET}^a$ ( $m^2g^{-1}$ )	$D_p^b$ (nm)	$V_p$ ( $cm^3g^{-1}$ )
KIT-6	93.87	22.99	2.735	705	8.76	0.889
NH <sub>2</sub> -KIT-6	102.61	25.13	5.945	503	6.62	0.62
Ag/NH <sub>2</sub> -KIT-6(3.2)	119.23	29.21	8.865	315	5.74	0.46
Ag/NH <sub>2</sub> -KIT-6(7.1)	124.27	30.44	10.04	280	5.18	0.39

$S_{BET}$ , specific surface area;  $D_p$ , pore diameter;  $W_T$ , pore wall thickness [ $a_0 / \sqrt{2}$ , (where  $a_0 = \sqrt{6} a$ )]

<sup>a</sup> Values obtained from XRD studies.

<sup>b</sup> Values obtained from N<sub>2</sub>-adsorption results.

## (2) NH<sub>2</sub>-KIT-6

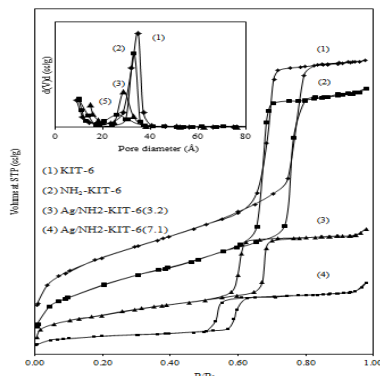


**Fig. 6:** Nitrogen adsorption/desorption and pore size distribution of KIT-6, NH<sub>2</sub>-KIT-6 and Ag/NH<sub>2</sub>-KIT-6 (2.5 & 7 %)

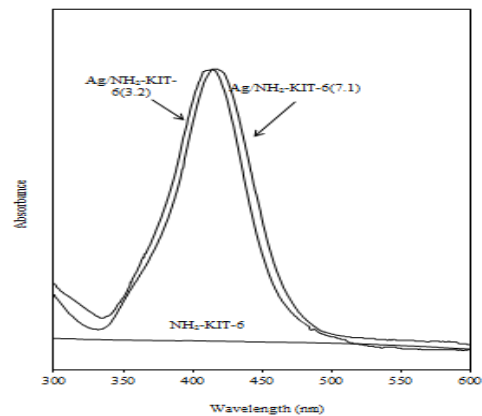


**Fig. 7:** UV-visible absorption spectra of NH<sub>2</sub>-KIT-6, Ag/NH<sub>2</sub>-

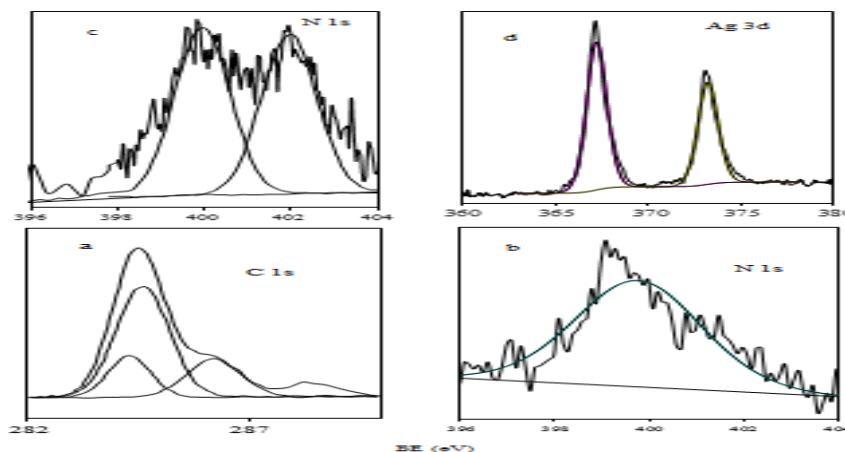


**Fig. 8:** XPS of a: C 1s, b& c: N 1s and d: Ag/NH<sub>2</sub>-KIT-6 (7 %) material.



### Antibacterial Activity

Antibiotic susceptibility test was performed against two bacterial strains, *S. aureus* as Gram positive & *Pseudomonas aeruginosa* as Gram negative strains **Table 2**. *Pseudomonas aeruginosa* was found to be resistant to Cefotaxime, Nalidixi acid and F while *S. aureus* was found to be resistant to Nalidixi acid and Sulfamethoxazole-trimethoprim. The antibacterial activity was affected with the concentrations 2.5 & 7% of Ag in Ag/NH<sub>2</sub>-KIT-6(x). The maximum inhibition zone diameter obtained is 33 and 30 mm when using 7 % against *P. aeruginosa* and *S. aureus* respectively.

**Shen et al. (2014)** the present results reported that the mesoporous Ag/NH<sub>2</sub>-KIT-6(x) exhibited good antibacterial activity and inhibited the growth of *P. aeruginosa* and *S. aureus* effectively. Whereas the mesoporous silica-KIT-6 and NH<sub>2</sub>-KIT-6 exhibited no bacterial inhibitory effects due to the absence of metal silver nanoparticles in the composite material. APTS modification procedure plays a very important role in the immobilization of silver nanoparticles onto mSiO<sub>2</sub>. Because the amino group of APTS could absorb a larger amount of Ag<sup>+</sup> ions tightly through the complex and electrostatic interactions between Ag<sup>+</sup> ions and amino functional groups. However, there only a small amount of Ag<sup>+</sup> ions could be absorbed onto mSiO<sub>2</sub> APTS modification and the created Ag nanoparticles could easily break away from the channels of mSiO<sub>2</sub> during the filtration and washing procedure. The synthesized AgNPs appeared to be highly dispersed on NH<sub>2</sub>-KIT6 and took the direction of KIT-6 pores, and the particle size distribution of mesoporous AgNPs was of 4-9 nm. In general, for nanoparticles to be effective, their typical size should not be larger than 50 nm. More precisely, mesoporous silver nanoparticles with size between 10 and 15 nm have increased stability, biocompatibility and enhanced antimicrobial activity (**Yacaman et al., 2001**). Some studies have revealed that the antibacterial action of AgNPs is more effective against *S. aureus* and *K. pneumoniae* when nanoparticles of smaller diameter (<30nm) are used (**Collins et al., 2010**).

**Morones et al. (2005)** The antibacterial effect of AgNPs as proposed is due to their smaller particles size that apparently has superior penetration ability into bacteria, especially in Gram-negative. Antimicrobial efficacy of AgNPs was evaluated by many researchers against a broad range of microbes, including MDR and non-MDR strains of bacteria, fungi, and viruses (**Malarkodi et al., 2013**).

**Rai et al. (2012)** Nano-sized metal particles are now well-established as a promising alternate to antibiotic therapy because they possess unbelievable potential for solving the problem associated with the development of multidrug resistance in pathogenic microorganisms, hence also regarded as next-generation antibiotics.



**Table 2:** Antibacterial activity of Ag/NH<sub>2</sub>-KIT-6(x) versus antibacterial activity of standard antibiotics against *S. aureus* and *P. aeruginosa*.

Antibacterial agent	Inhibition zone (mm)	
	<i>S. aureus</i>	<i>P. aeruginosa</i>
Ag/NH <sub>2</sub> -KIT-6 (7%)	30.0±0.0a	33.0±2.0a
Ag/NH <sub>2</sub> -KIT-6 (2.5%)	24.0±0.0bc	25.0±0.0b
Cefotaxime	13.0±0.0d	0.0±0.0f
Ceftriaxone	29.0±1.0a	17.0±0.0d
Amikacin	23.0±0.0bc	20.0±0.0c
Nalidixi acid	0.0±0.0e	0.0±0.0f
Neomycin	21.0±1.0bc	15.3±0.6e
Sulfamethoxazole-trimethoprim	0.0±0.0e	17.0±0.0d
Ampicillin	24.0±1.0b	17.0±0.0d
Colifuran	18.7±8.1c	0.0±0.0f
<b>F value</b>	<b>50.671***</b>	<b>844.590***</b>

The antimicrobial activity of Ag/NH<sub>2</sub>-KIT-6 (x) was also evaluated using the macrodilution broth susceptibility method. MIC and MBC of silver nanoparticles shown best results with the concentration 7 % of Ag/NH<sub>2</sub>-KIT-6 than the concentration 2.5 % of Ag/NH<sub>2</sub>-KIT-6 (**Table 3**). The MIC and MBC for the Ag /NH<sub>2</sub>-KIT-6 (2.5%) against tested bacteria *P. aeruginosa* and *S. aureus* differ in their values, but MIC equals MBC at the concentration (7%).

The concentration of Ag/NH<sub>2</sub>-KIT-6 (7%) shows 0.0045 and 0.041µl/ml for both MIC and MBC against *P. aeruginosa* and *S. aureus* respectively, i.e. completely inhibited, which indicated that the MIC and MBC of Ag/NH<sub>2</sub>-KIT-6(7%) are equal (**Table 3**). The obtained result agree with **Ansari et al. (2011)** whom showed that the AgNPs of 5–10 nm dimension display both bacteriostatic as well as bactericidal effects against *S. aureus*, MSSA and MRSA.

Gram-negative bacteria are more sensitive against nano Ag/NH<sub>2</sub>KIT-6 than gram-positive bacteria, also **Klapiszewski et al. (2015)** and **Yuan et al. (2017)** demonstrated that, AgNPs were more effective against Gram-negative *P. aeruginosa* than Gram-positive *S. aureus*, which could be explained by differences in membrane structure and the cell wall composition, which influence bacterial susceptibility to AgNPs.





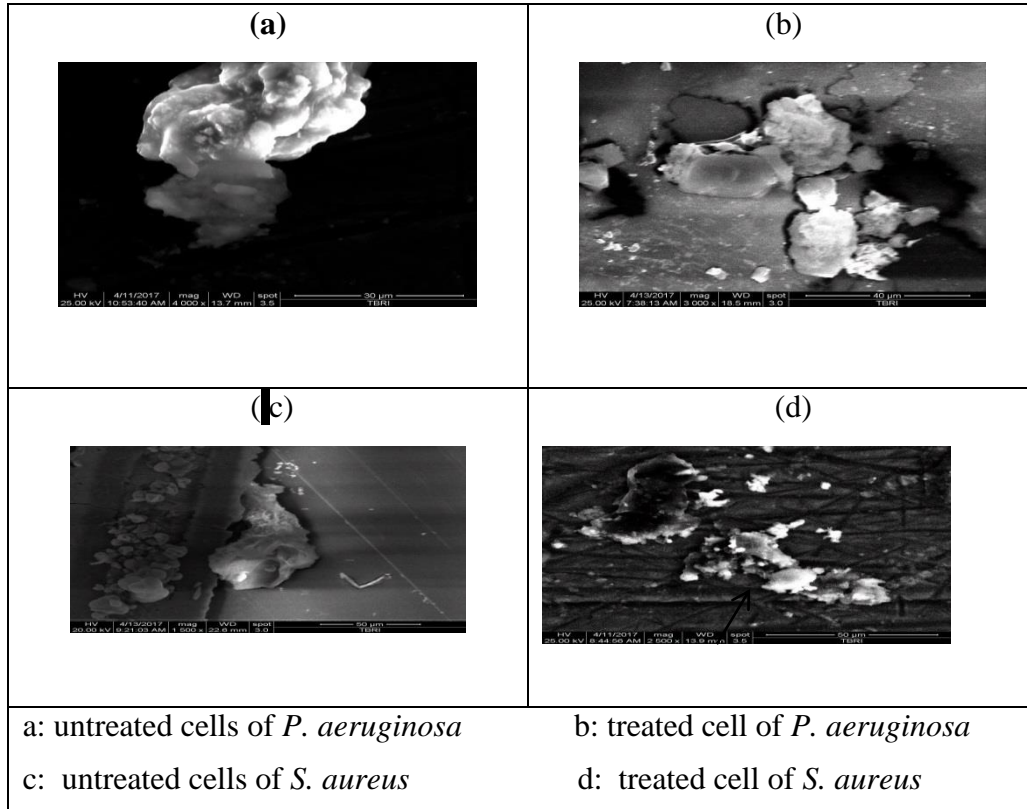
**Table 3:** The MIC and MBC of mesoporous silver nanoparticles (2.5 and 7%) against *P. aeruginosa* and *S.aureus*.

Ag/NH <sub>2</sub> -KIT-6 (x) (µg/ml)		Tested Bacterial	
		<i>P. aeruginosa</i>	<i>S.aureus</i>
2.5%	MIC	0.0045	0.041
	MBC	0.013	0.37
7%	MIC	0.0045	0.041
	MBC	0.0045	0.041

According to the obtained results, Mesoporous Ag/NH<sub>2</sub>-KIT-6 (7 %) exhibited excellent antibiofilm activity and prevented biofilm formation by *P.aeruginosa* and *S. aureus* qualitatively by micropate method **Fig 10**. Similar results were also reported by **Kalishwaralal et al. (2010)** against *P. aeruginosa* and *S. epidermidis* biofilms and found that 100 nM of AgNPs resulted in a95–98 % reduction in biofilm. **Thirumurugan et al. (2016)** reported that silver nanoparticles mostly had an inhibitory on biofilm formation as an average of  $60.67 \pm 2.52$  against *E.coli* followed by  $40.33 \pm 5.033$  for *P.aeruginosa* and  $34.33 \pm 9.71$  against *S. aureus* were obtained.



**Fig. 10:** SEM micrographs of mesoporous Ag/NH<sub>2</sub>-KIT-6 (7%) on the biofilm formation of *P. aeruginosa* and *S. aureus* cells.



## Conclusion

In this study, Antibacterial activity of mesoporous Ag/NH<sub>2</sub>-KIT-6(x) nanoparticles has been demonstrated in several investigations, In the present study, mesoporous nanoparticles showed good antibacterial activity against all the tested pathogens comparison with standard antibiotics . The results of MIC and MBC tests revealed a higher MIC value for *P. aeruginosa* comparing to the other tested pathogens. This may be due to the differences in bacterial cell walls, since Gram-negative bacteria have thinner cell wall comparing to Gram-positive bacteria. In agreement, **Kim et al.** However, in our study, the MBC values were identical for all the pathogens. It has been previously stated that bactericidal property of mesoporous nanoparticles is dependent on the concentration and size of nanoparticles and also the initial bacterial concentration. **Guilhelmelli, et al. (2013)** The susceptibility to a biocide varies markedly between planktonic cells and biofilms. Biofilms are microbial communities consisting of cells attached to biotic or abiotic surfaces, embedded in an exopolymeric matrix. These structures are well known for their remarkable resistance to diverse chemical, physical, and biological antimicrobial agents and are one of the main causes of persistent infections. Nanotechnology may provide the answer to penetrate such biofilms and reduce biofilm formation by the use of “nanofunctionalization” surface techniques to prevent the biofilm formation.



## References

- Abbaszadegan, A.; Ghahramani, Y.; Gholami, A.; Hemmateenejad, B.; Dorostkar, S. ; Nabavizadeh, M. and Sharghi, H.(2015):** The Effect of Charge at the Surface of Silver Nanoparticles on Antimicrobial Activity against Gram-Positive and Gram-Negative Bacteria: A Preliminary Study.
- Chen, M.; He, X.; Wang, K.; He, D.; Yang, S.; Qiu, P. and Chen, S. (2014):** A pH-responsive polymer/mesoporous silica nanocontainer linked through an acid cleavable linker for intracellular controlled release and tumor therapy *in vivo* . J. Mater. Chem. B **2**: 428–36.
- Christensen, G. D.; Simpson, W. A.; Bisno, A. L. and Beachey, E. H. (1985):** Adherence of slime producing strains of *Staphylococcus epidermidis* to smooth surfaces. Journal of Infection and Immunity, **37(1): 318-326**.
- Coates, J. (2000):** Interpretation of infrared spectra: A practical approach, R. A. Meyers, ed., Encyclopedia of Analytical Chemistry, W. John & Sons Ltd, Chichester, pp. **10815-10837**.
- Collins, T. L.; Markus, E. A.; Hassett, D. J. and Robinson, J. B. (2010):** The effect of a cationic porphyrin on *Pseudomonas aeruginosa* biofilms. Curr. Microbiol. **61**: 411–416.
- EL-Batal, A.I.; Amin, M.A.; Shehata, M.M.K. and Hallol, M. (2013):** Synthesis of Silver nanoparticles by *Bacillus stearothermophilus* using Gamma Radiation and their antimicrobial activity. World Appl. Sci. J. **22 (1): 01-16**.
- Feng, Q.L.; Wu, J.; Chen, G.Q.; Cui, F.Z.; Kim, T.N. and Kim, J.O. (2000):** A mechanistic study of the antibacterial effect of Silver ions on *Escherichia coli* and *Staphylococcus aureus*. J. Biomed. Mater. Res. **4**: 662-8.
- Ferraria, A.M.; Boufi, S.; Battaglini, N.; Botelho do Rego, A.M. and ReiVilars, M. (2010):** Hybrid systems of Silver nanoparticles generated on cellulose surfaces. Langmuir, **26(3): 1996-2001**.
- Franci, G.; Falanga, A.; Galdiero, S.; Palomba, L. ; Rai, M.; Morelli, G.; and Galdiero, M. (2015):** Silver nanoparticles as potential antibacterial agents. Molecules, **20**: 8856-8874.
- Gebeyehu, M.B.; Chang, Y. Abay, A.K.; Chang, S.; Lee, J.; Wu, C.; Chiang, T. and Murakami, R. (2016):** Fabrication and characterization of continuous silver nanofiber/polyvinylpyrrolidone (AgNF/PVP) core-shell nanofibers using the coaxial electrospinning process. RSC Advances, **6(59): 54162-54168**.
- Grigor'eva, A.; Saranina, I.; Tikunova, N.; Safonov, A.; Timoshenko, N. and Rebrov, A. and Ryabchikov, E. (2013):** Fine mechanisms of the interaction of Silver nanoparticles with the cells of *Salmonella typhimurium* and *Staphylococcus aureus*. Biometals, **26(3):479–488**.
- Guilhelmelli, F.; Vilela, N.; Albuquerque, P.; Derengowski, L. S.; Silva-Pereira, I. and Kyaw, C. M. (2013):** Antibiotic development challenges: the various mechanisms of action of antimicrobial peptides and of bacterial resistance. Frontiers in Microbiology, **9: 1-12**.
- Hassan , H.M.A.; Saad, E.M.; Soltan, M.S.; Betiha, M.A.; Butler, I.S. and Mostafa S.I. (2014):** A Palladium (II) 4-hydroxysalicylidene Schiff-base complex anchored on functionalized MCM-41: An efficient heterogeneous catalyst for the epoxidation of olefins. App. Catal. A. **488**: 148-159.



- Hassan, H.M.A.; Betiha, M.A.; Khder, S.; Mostafa, M. and Gallab, M. (2016):** Hafnium pentachloride ionic liquid for isomorphous and postsynthesis of HfKIT-6 mesoporous Silica: catalytic performances of Pd/SO<sub>4</sub><sup>2-</sup>/HfKIT-6. *J. Porous. Mater.* **23:** 1339-1351.
- Iconaru, S.L.; Prodan, A.M.; Le Coustumer, P. and Predoi, D. (2012):** Synthesis and antibacterial and antibiofilm activity of Iron Oxide Glycerol nanoparticles obtained by coprecipitation method. *J. Chemist.* **2013(2013):** 1-6.
- Kalishwaralal, K.; BarathManiKanth, S.; Pandian, S. R. K.; Deepak, V. and Gurunathan, S. (2010)** Silver nanoparticles impede the biofilm formation by *Pseudomonas aeruginosa* and *Staphylococcus epidermidis*. *Colloids Surf, B* **79:**340–344.
- Kheiralla, Z.M.H.; Rushdy, A. A.; Betiha, M.A. and Yakob N. A.N. (2014):** High-performance antibacterial of montmorillonite decorated with silver nanoparticles using microwave assisted method. *J. Nanopart. Res.* **16:**2560.
- Kim, K.; Kim, H.S. and Park, H.K. (2006):** Facile method to prepare surface-enhanced-Raman-scattering-active Ag nanostructures on silica spheres. *Langmuir*, **22:** 8083-8088.
- Klapiszewski, L.; Rzemieniecki, T.; Krawczyk, M.; Malina, D.; Norman, M.; Zdarta, J.; Majchrzak, I.; Dobrowolska, A.; Czaczyk, K. and Jesionowski, T. ( 2015):** Kraft lignin/silica-AgNPs as a functional material with antimicrobial activity. *Colloids. Surf. B Biointerfaces*, **134:**220-228.
- Klevens, R.M.; Morrison, M.A.; Nadle, J.; Petit, S.; Gershman, K.; Ray, S.; Harrison, L.H.; Lynfield, R.; Dumyati, G. and Townes, J.M.( 2007):** Invasive methicillin-resistant *Staphylococcus aureus* infections in the United States. *JAMA.* **298:** 1763–1771.
- Han, F.; Bai, Y.; Lin, R.; Yad, B.; Qi, Y.; Lun, N. and Zhang, J. (2011):** Template-Free Synthesis of Interconnected Hollow Carbon Nanospheres for High-Performance Anode Material in Lithium-Ion Batteries. *Adv. Energy Mater.* **1(5):** 798-801.
- Malarkodi, C.; Rajeshkumar, S.; Paulkumar, K.; Gnana Jobitha, G.; Vanaja, M. and Annadurai, G. (2013):** Biosynthesis of semiconductor nanoparticles by using sulfur reducing bacteria *Serratia nematodiphila*. *Adv. Nano. Res.* **1:** 83–91.
- McCusker, L. B. and Baerlocher, C. (2001):** In introduction to Zeolite Science and practice, H. Van Bekkum, E. M. Flanigen, P. A. Jacobs, and J. C. Jansen, eds. Amsterdam: Elsevier, pp. 137, 37.
- Morones, J. R.; Elechiguerra, J. L.; Camacho, A.; Holt, K.; Kouri, J. B.; Ramírez, J. T. and Yacaman, M. J. (2005):** The bactericidal effect of silver nanoparticles. *Nanotechnology*, **16:** 2346–2353.
- Natarajan, S. K. and Selvaraj, S. (2014):** Mesoporous Silica nanoparticles: importance of surface modifications and its role in drug delivery. *RSC Adv.* **4:** 14328–14334.
- Qasim, M.; Ananthaiah, J.; Dhara, S.; Paik, P. and Das, D. (2014):** Synthesis and characterization of ultra-fine colloidal Silica nanoparticles *Adv. Sci. Eng. Med.* **6:** 965–973.



- Qian, L.; Ren, Y.; Liu, T.; Pan, D.; Wang, H. and Chen, G. (2012):** Influence of KIT-6's pore structure on its surface properties evaluated by inverse gas chromatography. *Chem. Eng. J.* **213** : 186-194.
- Rai, M. and Duran, N. (2011):** Metal nanoparticles in microbiology, Springer-Verlag. Berlin Heidelberg.
- Rai, M.K.; Deshmukh, S.D.; Ingle, A.P. and Gade, A.K. (2012):** Silver nanoparticles: The powerful nanoweapon against multidrug-resistant bacteria. *J. Appl. Microbiol.* **112**: 841–852.
- Rai, M.; Deshmukh, S.D.; Ingle, A.P.; Gupta, I.R.; Galdiero, M. and Galdiero, S. (2016):** Metal nanoparticles: The protective nanoshield against virus infection. *Crit. Rev. Microbiol.* **24(1)**: 46-56.
- Karthikeyan, R.; Amaechi, B.T.; Rawls, H.R. and Lee, V.A. (2011):** Antimicrobial activity of nanoemulsion on cariogenic *Streptococcus mutans*. *Arch. Oral Biol.* **56**:437–445.
- Ruedas-Rama, M. J.; Walters, J. D.; Orte, A. and Hall, E. A. H. (2012):** Fluorescent nanoparticles for intracellular sensing: A review. *Anal. Chim. Acta*, **751**: 1–23.
- Ruparelia, J. P.; Chatterjee, A. K.; Duttagupta, S. P. and Mukherji, S. (2008):** Strain specificity in antimicrobial activity of Silver and Copper nanoparticles. *Acta Biomater.* **4(3)**: 707-716.
- Sajab, M.S.; Chia, C.H.; Zakaria, S.; Jani, S.M.; Ayob, M.K.; Chee, K.L.; Khiew, P.S. and Chiu, W.S. (2011):** Citric acid modified kenaf core fibres for removal of methylene blue from aqueous solution. *Bioresour. Technol.* **102**: 7237-7243.
- Shen, Q. J.; Wang, H.; Yang, X.; Ding, Z.; Luo, H.; Wang, C.; Pan, J.; Sheng, and Cheng, D. (2014):** *J. Non-Cryst. Solids*, **391**: 112–116.
- SPSS (2006).** SPSS base 15.0 User's guide. SPSS inc., Chicago, USA.
- Sweet, M.J. and Singleton, I. (2011):** Silver nanoparticles: A microbial perspective. *Adv. Appl. Microbiol.* **77**: 115–133.
- Taraszkiewicz, A.; Fila, G.; Grinholc, M. and Nakonieczna, J. (2012):** Innovative strategies to overcome biofilm resistance. *Biomed. Res. Int.* **2013 (2013)**: 1-13.
- Thirumurugan, G. J. V.; N. Seshagiri Rao, L. and Dhanaraju, M. D. (2016):** Elucidating pharmacodynamic interaction of silver nanoparticle - topical deliverable antibiotics. 15-745.
- Walker, B.; Barrett, S.; Polasky, S.; Galaz, V.; Folke, C.; Engstrom, G.; Ackerman, F.; Arrow, K.; Carpenter, S.; Chopra, K.; Daily, G.; Ehrlich, P.; Hughes, T.; Kautsky, N.; Levin, S.; Maler, K.G.; Shogren, J.; Vincent, J.; Xepapadeas, T. and de Zeeuw, A. (2009):** Environment. Looming global-scale failures and missing institutions. *Science*, **325**: 1345–1346.
- Wang, X.; Tseng, Y.; Chan, J.C.C. and Cheng, S. (2005):** Catalytic applications of aminopropylated mesoporous Silica prepared by a template-free route in flavanones synthesis. *J. Catal.* **233**: 266-275.
- Weber, C.; Coester, C.; Kreuter, J. and Langer, K. (2000):** Desolvation process and surface characterisation of protein nanoparticles. *Int. J. Pharm.* **194**: 91-102.
- Wu, S.; Mou, C. and Lin, H. (2013):** Synthesis of mesoporous silica nanoparticles. *Chem. Soc. Rev.* **42** : 3862–3875.



**Xia, T.; Kovichich, M.; Liang, M.; Meng, H.; Kabehie, S.; George, S.; Zink, J.I. and Nel, A.E. (2009):** Polyethyleneimine coating enhances the cellular uptake of mesoporous silica nanoparticles allowed safe delivery of siRNA and DNA constructs. *ACS Nano*. **3(10):**3273-3286.

**Vithiya, K.; Kumar, R. and Sen, S. (2014):** Bacillus sp. Mediated extracellular synthesis of silver nanoparticles. *Int. J. Pharm. Sci.* **6:525-7**

**Yacaman, M. J.; Ascencio, J. A.; Liu, H. B. and Gardea-Torresdey, J. (2001):** Structure shape and stability of nanometric sized particles. *J. Vacuum. Sci. Technol. B. Microelectron. Nanometer. Struct.* **19:** 1091–1103.

**Yildirim, A.; Demirel, G. B.; Erdem, R.; Senturk, B.; Tekinay, T. and Bayindir, M. (2013):** Pluronic polymer capped biocompatible mesoporous Silica nanocarriers. *Chem. Commun.* **49:** 9782–9784.

**Yuan, Y.; Peng, Q. and Gurunathan, S. (2017):** Effects of Silver nanoparticles on multiple drug-resistant strains of *Staphylococcus aureus* and *Pseudomonas aeruginosa* from mastitis-infected goats: An alternative approach for antimicrobial therapy. *Int. J. Mol. Sci.* **18:** 569.



## الفهرس

الصفحة	اسم الباحث	عنوان البحث	ر.ت
1-23	يونس يوسف أبونايجي	وضع الضاهر موضع الضمير ودلالته على المعنى عند المفسرين	1
24-51	محمد خليفة صالح خليفة محمود الجداوي	دراسة استقصائية حول مساهمة تقنية المعلومات والاتصالات في نشر ثقافة الشفافية ومحاربة الفساد	2
52-70	Ebtisam Ali Haribash	An Interactive GUESS Method for Solving Nonlinear Constrained Multi-Objective Optimization Problem	3
71-105	احمد علي الهادي الحويج احمد محمد سليم معوال	العوامل الخمسة الكبرى للشخصية وعلاقتها بالذكاء الوجداني لدى طلبة مرحلة التعليم الثانوي	4
106-135	محمد عبد السلام دخيل	في المجتمع الليبي التحضر وانعكاساته على الحياة الاجتماعية "دراسة ميدانية في مدينة الخمس"	5
136-158	سالم فرج زويبيك	الاستعارة التهكمية في القرآن الكريم	6
159-173	أسماء جمعة القلعي	دور الرياضات العملية الصوفية في تهذيب السلوك	7
174-183	S. M. Amsheri N. A. Abouthferah	On Coefficient Bounds for Certain Classes of Analytic Functions	8
184-191	N. S. Abdanabi	Fibrewise Separation axioms in Fibrewise Topological Group	9
192-211	Samah Taleb Mohammed	Investigating Writing Errors Made by Third Year Students at the Faculty of Education El-Mergib University	10
212-221	Omar Ali Aleyan Eissa Husen Muftah AL remali	SOLVE NONLINEAR HEAT EQUATION BY ADOMIAN DECOMPOSITION METHOD [ADM]	11
222-233	حسن احمد قرقد عبدالباسط محمد قريصة مصطفى الطويل	قياس تركيز بعض العناصر الثقيلة في المياه الجوفية لمدينة مصراته	12
234-244	ربيعة عبد الله الشبير عائشة أحمد عامر عبير مصطفى الهصيك	تعادم الدوال الكروية المناظرة لقيم ذاتية على سطح الكرة	13
245-255	Khadiga Ali Arwini Entisar Othman Laghah	$\lambda$ -Generalizations And $g$ - Generalizations	14



256-284	خيري عبدالسلام حسين كليب عبدالسلام بشير اشتيوي بشير ناصر مختار كصارة	Impact of Information Technology on Supply Chain management	15
285-294	Salem H. Almadhun, Salem M. Aldeep, Aimen M. Rmis, Khairia Abdulsalam Amer	Examination of 4G (LTE) Wireless Network	16
295-317	نور الدين سالم فريبع	التجربة الجمالية لدى موريس ميرلوبوتي	17
318-326	ليلى منصور عطية الغويج هدى على التقبي	Effect cinnamon plant on liver of rats treated with trichloroethylene	18
327-338	Fuzi Mohamed Fartas Naser Ramdan Amaizah Ramdan Ali Aldomani Husamaldin Abdualmawla Gahit	Qualitative Analysis of Aliphatic Organic Compounds in Atmospheric Particulates and their Possible Sources using Gas Chromatography Mass Spectrometry	19
339-346	E. G. Sabra A. H. EL- Rifae	Parametric Tension on the Differential Equation	20
347-353	Amna Mohamed Abdelgader Ahmed	Totally Semi-open Functions in Topological Spaces	21
354-376	زينب إمام أبو راس حواء بشير بالنور	كتاب الخصائص لابن جني دراسة بعض مواضع الحذف من ت"392" المسمى: باب في شجاعة العربية	22
377-386	لطيفة محمد الدالي	Least-Squares Line	23
387-397	نادية محمد الدالي ايمان احمد اخميرة	THEORETICAL RESEARCH ON AI TECHNOLOGIES FOR LEARNING SYSEM	24
398-409	Ibrahim A. Saleh Tarek M. Fayez Mustafah M. A. Ahmad	Influence of annealing and Hydrogen content on structural and optoelectronic properties of Nano-multilayers of a-Si:H/a-Ge: H used in Solar Cells	25
410-421	أسماء محمد الحبشي	The learners' preferences of oral corrective feedback techniques	26
422-459	أمينة محمد العكاشي ربيعة عثمان عبد الجليل عفاف محمد بالحاج فتحية علي جعفر	التقدير الإيجابي المسبق لفاعلية الذات ودوره في التغلب على مصادر الضغوط النفسية " دراسة تحليلية "	27





460-481	Aisha Mohammed Ageal Najat Mohammed Jaber	English Pronunciation problems Encountered by Libyan University Students at Faculty of Education, Elmergib University	28
482-499	الحسين سليم محسن	The Morphological Analysis of the Quranic Texts	29
500-507	Ghada Al-Hussayn Mohsen	Cultural Content in Foreign Language Learning and Teaching	30
508-523	HASSAN M. ALI Mostafa M Ali	The relationship between <i>slyA</i> DNA binding transcriptional activator gene and <i>Escherichia coli</i> fimbriae and related with biofilm formation	31
524-533	Musbah A. M. F. Abduljalil	Molecular fossil characteristics of crude oils from Libyan oilfields in the Zalla Trough	32
534-542	سعدون شهبوب محمد	تلوث المياه الجوفية بالنترات بمنطقة كعام، شمال غرب ليبيا	33
543-552	Naima M. Alsharif Mahmoud M. Buazzi	Analysis of Genetic Diversity of <i>Escherichia Coli</i> Isolates Using RAPD PCR Technique	34
553-560	Hisham mohammed alnaib alshareef aisha mohammed elfagaeh aisha omran alghawash abdualaziz ibrahim lawej safa albashir hussain kaka	The Emergence of Virtual Learning in Libya during Coronavirus Pandemic	35
561-574	Abdualaziz Ibrahim Lawej Rabea Mansur Milad Mohamed Abduljalil Aghnayah Hamza Aabeed Khalafllaa <sup>3</sup>	ATTITUDES OF TEACHERS AND STUDENTS TOWARDS USING MOTHER TONGUE IN EFL CLASSROOMS IN SIRTE	36
575-592	صالحة التومي الدروقي أمال محمد سالم أبوسته	دافع الانجاز وعلاقته بالرضا الوظيفي لدى معلمي مرحلة التعليم الأساسي "ببلدية ترهونة"	37
593-609	آمنة سالم عبد القادر قدورة نجية علي جبريل انبية	الإرشاد النفسي ودوره في مواجهة بعض المشكلات الأخرية الراهنة	38
610-629	Hanan B. Abousittash, Z. M. H. Kheiralla Betiha M.A.	Effect Mesoporous silica silver nanoparticles on antibacterial agent Gram- negative <i>Pseudomonas</i> <i>aeruginosa</i> and Gram-positive <i>Staphylococcus</i> <i>aureus</i>	39
630-652	حنان عمر بشير الرمالي	برنامج التربية العملية وتطويره	40
653-672	Abdualla Mohamed Dhaw	Towards Teaching CAT tools in Libyan Universities	41



673-700	عثمان علي أميمن سليمة رمضان الكوت زهرة عثمان البرق	سبل إعادة أعمار وتأهيل سكان المدن المدمرة بالحرب ومعوقات المصالحة الوطنية في المجتمع الليبي: مقارنة نفس-اجتماعية	42
701-711	Abdulrhman Mohamed Egnebr	Comparison of Different Indicators for Groundwater Contamination by Seawater Intrusion on the Khoms city, Libya	43
712-734	Elhadi A. A. Maree Abdualah Ibrahim Sultan Khaled A. Alurffi	Hilbert Space and Applications	44
735-759	معتوق علي عون عمار محمد الزليطني عرفات المهدي قرينات	الموارد الطبيعية اللازمة لتحقيق التنمية الاقتصادية بشمال غرب ليبيا وسبل تحقيق الاستدامة	45
760-787	سهام رجب العطوي هدى المبروك موسى	الخلج وعلاقته بمفهوم الذات لدى تلاميذ الشق الثاني بمرحلة التعليم الاساسي بمنطقة جنزور	46
788-820	هنية عبدالسلام بالوص زهرة المهدي أبو راس	الصلابة النفسية ودورها الوقائي في مواجهة الضغوط النفسية	47
821-847	عبد الحميد مفتاح أبو النور محي الدين علي المبروك	ودوره في الحد من التمر التوجيه التربوي والإرشاد النفسي المدرسي	48
848	الفهرس		52